Transition mode long period grating biosensor with functional multilayer coatings

Pierluigi Pilla,[1] Viera Malachovská,[2] Anna Borriello,[2] Antonietta Buosciolo,[2] Michele Giordano,[2,*] Luigi Ambrosio,[2] Antonello Cutolo,[1] and Andrea Cusano[1]

[1] *Optoelectonic Division, Engineering Department, University of Sannio, Benevento, Italy*
[2] *Institute for Composite and Biomedical Materials, National Research Council (IMCB-CNR), Napoli, Italy*
**gmichele@unina.it*

Abstract: We report our latest research results concerning the development of a platform for label-free biosensing based on overlayered Long Period Gratings (LPGs) working in transition mode. The main novelty of this work lies in a multilayer design that allows to decouple the problem of an efficient surface functionalization from that of the tuning in transition region of the cladding modes. An innovative solvent/nonsolvent strategy for the dip-coating technique was developed in order to deposit on the LPG multiple layers of transparent polymers. In particular, a primary coating of atactic polystyrene was used as high refractive index layer to tune the working point of the device in the so-called transition region. In this way, state-of-the-art-competitive sensitivity to surrounding medium refractive index changes was achieved. An extremely thin secondary functional layer of poly(methyl methacrylate-co-methacrylic acid) was deposited onto the primary coating by means of an original identification of selective solvents. This approach allowed to obtain desired functional groups (carboxyls) on the surface of the device for a stable covalent attachment of bioreceptors and minimal perturbation of the optical design. Standard 1-ethyl-3-(3-dimethylaminopropyl)carbodiimide / N-hydrosuccinimide (EDC / NHS) coupling chemistry was used to link streptavidin on the surface of the coated LPG. Highly sensitive real-time monitoring of multiple affinity assays between streptavidin and biotinylated bovine serum albumin was performed by following the shift of the LPGs attenuation bands.

OCIS codes: (350.2770) Gratings; (060.2370) Fiber optics sensors; (240.0310) Thin films; (280.1415) Biological sensing and sensors.

References and links

1. X. Fan, I. M. White, S. I. Shopova, H. Zhu, J. D. Suter, and Y. Sun, "Sensitive optical biosensors for unlabeled targets: a review," Anal. Chim. Acta **620**(1-2), 8–26 (2008).
2. S. W. James, and R. P. Tatam, "Optical fibre long-period grating sensors: characteristics and application," Meas. Sci. Technol. **14**(5), R49–R61 (2003).
3. R. Falciai, A. G. Mignani, and A. Vannini, "Long period gratings as solution concentration sensors," Sens. Actuators B Chem. **74**(1-3), 74–77 (2001).
4. M. P. DeLisa, Z. Zhang, M. Shiloach, S. Pilevar, C. C. Davis, J. S. Sirkis, and W. E. Bentley, "Evanescent wave long-period fiber bragg grating as an immobilized antibody biosensor," Anal. Chem. **72**(13), 2895–2900 (2000).
5. N. D. Rees, S. W. James, R. P. Tatam, and G. J. Ashwell, "Optical fiber long-period gratings with Langmuir-Blodgett thin-film overlays," Opt. Lett. **27**(9), 686–688 (2002).
6. I. Del Villar, I. Matías, F. Arregui, and P. Lalanne, "Optimization of sensitivity in Long Period Fiber Gratings with overlay deposition," Opt. Express **13**(1), 56–69 (2005).
7. A. Cusano, A. Iadicicco, P. Pilla, L. Contessa, S. Campopiano, A. Cutolo, and M. Giordano, "Cladding mode reorganization in high-refractive-index-coated long-period gratings: effects on the refractive-index sensitivity," Opt. Lett. **30**(19), 2536–2538 (2005).
8. Z. Wang, J. Heflin, R. Stolen, and S. Ramachandran, "Analysis of optical response of long period fiber gratings to nm-thick thin-film coating," Opt. Express **13**(8), 2808–2813 (2005).
9. A. Cusano, P. Pilla, M. Giordano, and A. Cutolo, "Modal Transition in Nano-Coated Long Period Fiber Gratings: Principle and Applications to Chemical Sensing," in *Advanced Photonic Structure for Biological and Chemical Detection*, X. Fan, Ed. (Springer, 2009).

#132072 - $15.00 USD Received 21 Jul 2010; revised 27 Sep 2010; accepted 27 Sep 2010; published 3 Jan 2011

10. P. Pilla, P. F. Manzillo, V. Malachovska, A. Buosciolo, S. Campopiano, A. Cutolo, L. Ambrosio, M. Giordano, and A. Cusano, "Long period grating working in transition mode as promising technological platform for label-free biosensing," Opt. Express **17**(22), 20039–20050 (2009).
11. D. W. Kim, Y. Zhang, K. L. Cooper, and A. Wang, "Fibre-optic interferometric immuno-sensor using long period grating," Electron. Lett. **42**(6), 324–325 (2006).
12. Z. Wang, J. R. Heflin, K. Van Cott, R. H. Stolen, S. Ramachandran, and S. Ghalmi, "Biosensors employing ionic self-assembled multilayers adsorbed on long-period fiber gratings," Sens. Actuators B Chem. **139**(2), 618–623 (2009).
13. X. Chen, L. Zhang, K. Zhou, E. Davies, K. Sugden, I. Bennion, M. Hughes, and A. Hine, "Real-time detection of DNA interactions with long-period fiber-grating-based biosensor," Opt. Lett. **32**(17), 2541–2543 (2007).
14. J. Yang, P. Sandhu, W. Liang, C. Xu, and Y. Li, "Label free fiber optic biosensors with enhanced sensitivity," IEEE J. Sel. Top. Quantum Electron. **13**(6), 1691–1696 (2007).
15. L. Rindorf, J. B. Jensen, M. Dufva, L. H. Pedersen, P. E. Høiby, and O. Bang, "Photonic crystal fiber long-period gratings for biochemical sensing," Opt. Express **14**(18), 8224–8231 (2006).
16. H. Shibru, Y. Zhang, K. L. Cooper, G. R. Pickrell, and A. Wang, "Optimization of layer-by-layer electrostatic self-assembly processing parameters for optical biosensing," Opt. Eng. **45**(2), 024401 (2006).
17. I. Del Villar, I. R. Matias, F. J. Arregui, and M. Achaerandio, "Nanodeposition of materials with complex refractive index in long-period fiber gratings," J. Lightwave Technol. **23**, 4192 (2005).
18. E. Davies, R. Viitala, M. Salomäki, S. Areva, L. Zhang, and I. Bennion, "Sol-Gel derived coating applied to long period gratings for enhanced refractive index sensing properties," J. Opt. A, Pure Appl. Opt. **11**(1), 015501 (2009).
19. J. M. Goddard, and J. H. Hotchkiss, "Polymer surface modification for the attachment of bioactive compounds," Prog. Polym. Sci. **32**(7), 698–725 (2007).
20. J. M. Corres, I. del Villar, I. R. Matias, and F. J. Arregui, "Two-layer nanocoatings in long-period fiber gratings for improved sensitivity of humidity sensors," IEEE Trans. NanoTechnol. **7**(4), 394–400 (2008).
21. I. Del Villar, I. R. Matias, and F. J. Arregui, "Deposition of coatings on long-period fiber gratings: tunnel effect analogy," Opt. Quantum Electron. **38**(8), 655–665 (2006).
22. K. Stoeffler, C. Dubois, A. Ajji, N. Guo, F. Boismenu, and M. Skorobogatiy, "Fabrication of all-polymeric photonic bandgap Bragg fibers using rolling of coextruded PS/PMMA multilayer films," Polym. Eng. Sci. **50**(6), 1122–1127 (2010).
23. H. Ma, A. K.-Y. Jen, and L. R. Dalton, "Polymer-Based Optical Waveguides: Materials, Processing, and Devices," Adv. Mater. **14**(19), 1339–1365 (2002).
24. D. Ennis, H. Betz, and H. Ade, "Direct spincasting of polystyrene thin films onto poly(methyl methacrylate)," J. Polym. Sci. Part B: Polym. Phys. **44**(22), 3234–3244 (2006).
25. M. J. E. Fischer, "Amine coupling through EDC/NHS: a practical approach," Methods Mol. Biol. **627**, 55–73 (2010).
26. A. Cusano, A. Iadicicco, P. Pilla, A. Cutolo, M. Giordano, and S. Campopiano, "Sensitivity characteristics in nanosized coated long period gratings," Appl. Phys. Lett. **89**(20), 201116 (2006).
27. P. Pilla, P. Foglia Manzillo, M. Giordano, M. L. Korwin-Pawlowski, W. J. Bock, and A. Cusano, "Spectral behavior of thin film coated cascaded tapered long period gratings in multiple configurations," Opt. Express **16**(13), 9765–9780 (2008).
28. F. Vollmer, D. Braun, A. Libchaber, M. Khoshsima, I. Teraoka, and S. Arnold, "Protein detection by optical shift of a resonant microcavity," Appl. Phys. Lett. **80**(21), 4057–4059 (2002).
29. B. Bhushan, D. R. Tokachichu, M. T. Keener, and S. C. Lee, "Morphology and adhesion of biomolecules on silicon based surfaces," Acta Biomater **1**(3), 327–341 (2005).
30. M. Unemori, Y. Matsuya, S. Matsuya, A. Akashi, and A. Akamine, "Water absorption of poly(methyl methacrylate) containing 4-methacryloxyethyl trimellitic anhydride," Biomaterials **24**(8), 1381–1387 (2003).
31. B. Spačková, M. Piliarik, P. Kvasnicka, C. Themistos, M. Rajarajan, and J. Homola, "Novel concept of multi-channel fiber optic surface plasmon resonance sensor," Sens. Actuators B Chem. **139**(1), 199–203 (2009).

1. Introduction

Biosensors development is a dynamic research field motivated by a vast number of possible applications such as fundamental biological research, drugs development, medical diagnostics, food quality testing and biohazard detection.

In recent years a considerable effort in this sector was devoted to the study of extremely sensitive refractive index (RI) transducers, mainly based on evanescent-wave probing of the surrounding medium, able to continuously monitor unlabeled biomolecular interactions occurring at their interface [1]. Label-free biosensing is undoubtedly attractive since it allows for recognition of target molecules in a single step and in their natural forms without the need for biological reporters as in fluorescence-based detection. It is widely recognized that labeling chemistries are time-consuming, require trained personnel and can interfere with an assay.

Long period fiber gratings (LPGs) are devices consisting of a periodic perturbation of a single mode fiber core and are basically in-fiber diffraction gratings generating co-

#132072 - $15.00 USD Received 21 Jul 2010; revised 27 Sep 2010; accepted 27 Sep 2010; published 3 Jan 2011

propagating cladding modes that probe the external medium in close proximity of the cladding surface via evanescent-wave [2]. LPGs are inherently sensitive to surrounding medium refractive index (SRI) changes and therefore have become increasingly popular devices for the implementation of chemical sensors and biosensors [3,4].

A strong impulse to this development was recently given by the integration of nano-scale polymer overlays and by the discovery of the modal transition phenomenon [5–8]. It is by now very well known that the SRI sensitivity of LPGs can be optimized at the desired working point through the deposition of a high refractive index (HRI) layer by acting on its thickness (ranging in hundreds of nanometers). Shifts of the spectral features as high as thousands of nanometers for a unitary change of SRI can be easily obtained and therefore LPGs coated by HRI functional layers have been successfully exploited for chemical and biomolecular sensing [9,10].

Although polymer coated LPGs for label-free biosensing were already explored by other authors, it should be underlined that in those works the HRI overlay served primarily as a substrate for bioreceptors immobilization rather than a mean knowingly used to optimize the device sensitivity [11,12]. The latter is more often increased by means of high order modes at the dispersion turning point, cladding etching, cascaded LPGs in Michelson configuration, fluid pushed through holes of a photonic crystal fiber LPG [13–15]. Moreover the real-time monitoring of biomolecular interactions is rarely reported.

The increase in sensitivity of label-free optical biosensors, even if primarily focused on the SRI sensitivity of the transducers, involves also the improvement of bioreceptors immobilization strategies. In ref [10]. the surface immobilization chemistry was based on the simple adsorption (hydrophobic interaction-driven) of biotinylated bovine serum albumin (bBSA) on a polystyrene overlay and the formation of the biotin-streptavidin complex was used as a benchmark to test the performance of the realized biosensor. However that approach is unpractical to use as a general immobilization technique. In fact, if one wants to link a bioreceptor on the sensor surface, an antibody for instance, there is anyway the need of the two intermediate protein layers (the bBSA and the streptavidin (SA)) and the bioreceptor to be immobilized must be pre-biotinylated. It is apparent how this way is time-consuming and costly and how it would be easier to directly and stably immobilize bioreceptors on the sensor surface through a covalent link with suitable functional groups. Surface immobilization chemistry for HRI overlays on LPGs is a delicate issue which should consider a concurrent approach taking into account the optical design of the device and the desired functionality of the interface.

Electrostatic self-assembly (ESA) deposition technique offers all the flexibility needed to have a precise control over the chemical composition and thickness of the overlay, but unfortunately it introduces detrimental optical losses affecting the attenuation bands visibility in the transition region [16,17]. Furthermore, this technique is very time consuming because it proceeds layer by layer of few nanometers at a time and tens of layers are needed to achieve an adequate coating thickness for a substantial improvement of the device sensitivity. Even metal oxide coatings have been investigated in this specific niche of LPG-based biosensors, for example it was shown that sol-gel derived TiO_2 coatings, as HRI coatings, can increase the sensitivity of LPGs while providing a biocompatible substrate for bioreceptors immobilization, however it was not demonstrated the tuning of the device in full transition region for aqueous environment [18].

Direct chemical modification of polymeric HRI overlays involves mostly wet chemical treatments, plasma treatments and UV irradiation [19]. These methods present some drawbacks for our purposes. In fact, chemical surface modification reactions can be difficult to control and may result in irregular etching, ionized gas treatments require costly and large infrastructures and increase surface roughness, UV light exposure may alter LPG characteristics as well as bulk polymer properties. Especially the increase in surface roughness discourages the use of a certain surface modification technique because it can greatly increase the optical losses of the overlay. Moreover all these techniques produce a broad spectrum of functional groups without ensuring high density of the desired functional group. On the other

#132072 - $15.00 USD Received 21 Jul 2010; revised 27 Sep 2010; accepted 27 Sep 2010; published 3 Jan 2011

side the use of bulk-functionalized polymers as overlay may result in unsuitable bulk characteristics (refractive index, hydrophilicity, etc.). It is therefore straightforward the need to implement a multilayer strategy where the first overlay serves to tune the working point of the device in the transition region while a second thinner overlay provides the specific function.

Some examples of this strategy have been already reported with reference to humidity sensing by exploiting the electrostatic self-assembly (ESA) technique [20]. In fact, hygrosensitive polymeric materials have usually too low refractive index (RI) to be used for the optimization of LPGs sensitivity. This is why they have to be deposited on the top of a passive primary HRI coating. As already observed, while ESA deposition technique is a versatile technique for the implementation of functional coatings with tailored properties it is also well recognized that they show a certain amount of optical loss which causes the fading of LPGs attenuation bands in full transition region [17]. Therefore a less sensitive working point of the device should be chosen to preserve attenuation bands visibility. On the other side dip-coating (DC) technique, while being a less accurate deposition technique, has demonstrated to be a good choice for the deposition of thin films with lower optical losses.

Moreover, the importance of being able to deposit multiple coaxial cylindrical layers of suitable thickness and refractive index contrast on optical waveguides goes beyond the specific application presented in this work. In fact, this can be a mean to finely tune the waveguide dispersion behaviour, of which the modal transition is just one expression, with interesting implications in different fields [21,22]. Polystyrene (PS) and poly-methyl-methacrylate (PMMA) are probably the most exploited polymers for optical waveguide fabrication so far [22,23]. They are inexpensive, easily processable and highly transparent. Finally, PS/PMMA multilayer structures, whose deposition with selective solvents is not so trivial as it might appear, have drawn considerable interest in recent years as a model system for a wide range of investigations [24].

In this work we propose a multilayer approach for the coating of the LPG in order to independently tune the working point in transition region and achieve an efficient surface functionalization without incurring the problem of the attenuation bands fading. Here we also report for the first time to the best of our knowledge the deposition of multiple highly transparent nano-scale polymer coatings on LPGs by adopting DC and a solvent/nonsolvent strategy. In particular we used ordinary atactic polystyrene (PS) as a primary HRI coating to tune the working point of the device in transition region. A secondary very thin layer of poly(methyl methacrylate-co-methacrylic acid) (PMMA-co-MA) was then deposited to provide a caroboxyl-containing surface minimizing at the same time its impact on the optical design of the device. Great emphasis was given to the discussion of the fabrication and characterization steps. The outer functional surface of the coated device was exploited for biomolecular experiments as a substrate for covalent immobilization of bioreceptors through commonly used NHS/EDC chemistry [25]. We also show successful monitoring of immobilization strategy and binding assay between covalently immobilized streptavidin (SA) and biotinylated bovine serum albumin (bBSA). Finally, improvement of sensitivity, attempt to device response equalization and detection of protein multilayers are also reported.

2. Theoretical background

Long period gratings consists of a periodic RI modulation in the core of a single mode optical fiber providing an efficient method for coupling the core mode to discrete forward propagating cladding modes at distinct wavelengths $\lambda_{res,0i}$ given by a phase matching condition

#132072 - $15.00 USD Received 21 Jul 2010; revised 27 Sep 2010; accepted 27 Sep 2010; published 3 Jan 2011

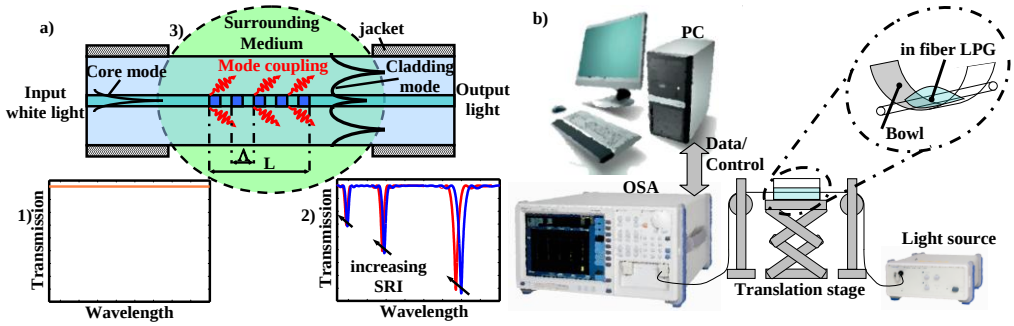

Fig. 1. (a) Pictorial description of mode coupling in LPGs and spectral dependence on SRI (not to scale): 1) spectrum of incoming white light; 2) spectrum of transmitted light at the output of the bare LPG, also showing the shift of the attenuation bands for increasing SRI; 3) LPG structure; (b) schematic of the experimental set-up.

$\lambda_{res,0i} = (n_{co}-n_{cl,0i}) \times \Lambda$ where n_{co} and $n_{cl,0i}$ are the core and i^{th} cladding mode effective indices respectively, Λ is the grating period. As a result of the mode coupling process, the LPG transmission spectrum shows several attenuation bands related to different excited cladding modes (see Fig. 1(a)).

LPGs are sensitive to a number of environmental parameters (temperature, strain, bending, SRI) which affect the phase matching condition changing, in turn, the spectral position of the attenuation bands [2]. However, appropriate simple countermeasures can be used to minimize the effect of the parameters not of interest. The dependence of LPGs spectral features on SRI changes is what makes them very attractive for chemical sensing and biosensing applications. It is by now a well established concept that the deposition of a HRI layer of few hundreds nanometers (depending on the RI of the overlay material) onto the cladding over the grating region drastically modifies the transfer characteristic and hence the sensitivity characteristic of the bare device [26]. The transfer characteristic of the coated device with respect to SRI changes can be very well described by a transition function such as a Lorentzian-Cumulative function. For a given material (fixed RI) and overlay thickness, when the SRI increases all the cladding modes effective indices increase following a transition function trend until they reach the effective index value originally displayed by the next lower order cladding mode. This is reflected through the phase matching condition in the shift of each attenuation band toward the position originally occupied by the next lower one. When the attenuation bands of the coated LPG are tuned in the middle of the spectral separation of two consecutive attenuation bands of the original bare device then we say that it is working in the transition region or in transition mode. LPGs working in transition mode have attenuation bands that exhibit a sensitivity ($|\partial\lambda_{res}/\partial SRI|$) of thousands of nanometers per refractive index unit (RIU). The tuning in transition region can be accomplished depending on the RI of the medium where the device should work by acting on the overlay thickness. Therefore the coated device can be used as biosensor if the overlay surface is properly functionalized in the way to specifically concentrate biomolecules which in turn produce localized refractive index changes.

3. Multilayer coated LPGs: fabrication and characterization

3.1 Fabrication

In this work two commercial LPGs were used for the experiments, namely grating A (Λ = 460 μm, L = 3 cm) and grating B (Λ = 380 μm, L = 3 cm). Grating A was already used for the experiments reported in ref [10]. and here it was once again exploited in order to do a comparison between the transfer characteristic of the single- and double-layer coated LPG. Grating B was used in this work to show the performance improvement when higher order modes are considered.

#132072 - $15.00 USD Received 21 Jul 2010; revised 27 Sep 2010; accepted 27 Sep 2010; published 3 Jan 2011

The DC technique was used to deposit a thin film of PS (M_w = 280,000, # 18242-7 Aldrich), whose bulk RI is about 1.59, onto the grating region. This deposition technique consists mainly of immersing the fiber with the LPG into a solution of the polymer and then of withdrawing it with a well-controlled speed. Before deposition the LPG was thoroughly cleaned in boiling chloroform. Deposition solution was 9.5% (w/w) of PS in chloroform (analytical grade 99.9, J.T. Baker). The DC was performed by means of an automated system at an extraction speed of 10 cm/min. The PS coated LPG was subsequently dip-coated into a solution 10% (w/w) PMMA-co-MA (M_w = 34,000; # 376914 Aldrich) in chloroform:isopropanol (1:3, v/v; analytical grade 99.9, J.T. Baker). Considering the relatively small amount (1.6%) of methacrylic acid in this PMMA co-polymer we assume its refractive index to be the same as the homopolymer, i.e. 1.49.

It is important at this point to highlight that the deposition of a second layer by DC implies the need for a solvent/nonsolvent strategy. In other words, the second layer should be deposited from a solution whose solvents would not damage the underlying layer.

Studies showing the complexity of the deposition of PS layers on PMMA by spin coating with selective solvents have been reported [24]. Here we have investigated our original approach to the deposition of a thin layer of PMMA-co-MA on PS by dip-coating. One important difficulty to consider in this system is that PS is an highly hydrophobic polymer while PMMA-co-MA has an hydrophilic nature, therefore the use of solvents with a higher polarity, with respect to chloroform, could prevent the good adhesion of the secondary layer and cause its slipping as well as dewetting defects, as it was experimentally verified in the case of acetone, acetic acid, ethanol:water (1:1, v/v), MEK:isopropanol (1:1). The problem was solved by using a mixture of solvents containing a small amount of a mutual solvent for both polymers, in our case chloroform, and a major part of mutual nonsolvent, in our case isopropanol, in a volumetric ratio 1:3. In this way the integrity of the first layer was preserved and good adhesion and uniformity of the secondary layer was ensured.

3.2 Characterization

After solvent evaporation the LPG was fixed straight, under constant strain and at controlled room temperature in a bowl. The optoelectronic set-up used for SRI characterization comprises a white light source of 400-1800 nm wavelength range and an optical spectrum analyzer (OSA, see Fig. 1(b)). The analysis was focused on the spectral range 1200-1700 nm. The SRI was changed by using aqueous glycerol solutions whose refractive indices were measured by an Abbe refractometer at 589 nm. Figure 2(a) shows the spectral position of the attenuation band related to the fourth cladding mode for the bare LPG A and for the coated device.

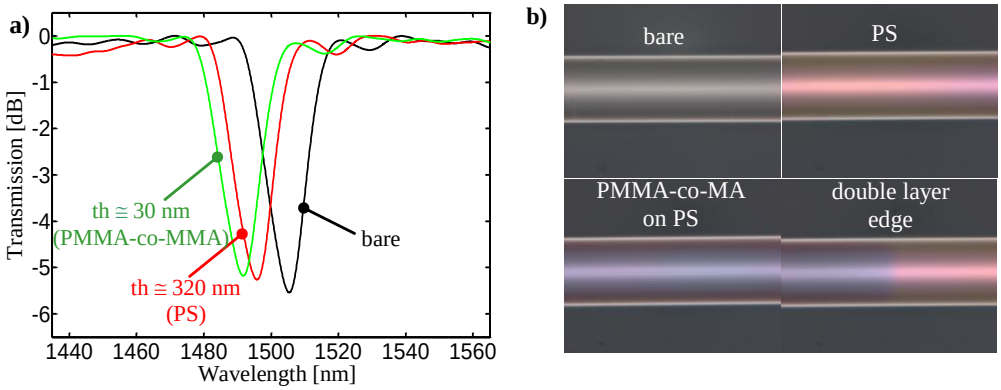

Fig. 2. a) Effect of the overlays deposition on the fourth order cladding mode attenuation band of grating A; b) optical microscopy images of a double-layer coated optical fiber. Clock wise: bare, PS (pink), transition from PS to PMMA-co-MA on PS, central zone with the double-layer of PMMA-co-MA on PS (violet).

#132072 - $15.00 USD Received 21 Jul 2010; revised 27 Sep 2010; accepted 27 Sep 2010; published 3 Jan 2011

In particular the resulting overlay thickness after DC from the 9.5% PS solution was ≅320 nm while the secondary layer obtained from the 10% PMMA-co-MA solution was estimated to be of few tens of nanometers (≅30 nm). They were inferred by previous deposition process characterizations through atomic force microscopy (AFM) for the first layer ([27]) and by numerical simulations for the second layer.

When an HRI overlay is deposited onto the grating the effective RI of the cladding modes is increased, as a consequence the attenuation bands experience a blue shift, that for the fourth order cladding mode in Fig. 2(a) is about 9.25 nm. The second layer of PMMA-co-MA produces a cumulative effect of 4.1 nm on the attenuation band shift. The goodness of the deposition process is also testified by the subsistence of the attenuation band visibility. In fact, a secondary layer with defects would determine a dramatic decrease of the attenuation band depth due to scattering losses [17]. In Fig. 2(b) are reported some optical microscopy images of an optical fiber coated with the polymer double-layer in different positions along the fiber axis. The pictures reveal smooth and homogenous layers. Since PS and PMMA-co-MA are transparent polymers, the apparent colours are due to interference of the light reflected back from the different interfaces.

The spectral characterization to SRI changes with the double-layer coated LPG for the fourth and fifth cladding modes in terms of attenuation bands minima position is reported in Fig. 3(a). In the same figure it is also reported a comparison to the SRI characterization of the same grating coated with a single PS layer of ≅320 nm thickness from ref [10]. This experimental step was performed in order to ascertain that the additional layer with lower refractive index would not have detrimental effects on the sensitivity characteristics of the device.

The presence of the thin PMMA-co-MA layer does not change the well know transition behaviour of the attenuation bands which move from their initial position to that initially related to the next lower order cladding mode by increasing the SRI [7]. Experimental data were fitted with a Lorentzian-Cumulative function which was already proven to be a good fitting for the modal transition in previous experiments [26]. The position of the attenuation band related to the fifth cladding mode in air can be only inferred by the fitting since it was out of the OSA spectral window. The resonance-shaped sensitivity characteristics of the coated device are reported in Fig. 3(b) for the fourth and fifth cladding modes and for the single- and double-layer coated LPG, as extrapolated from the experimental results. From this comparison and with reference to [10] it is apparent the effect of the additional outer layer is analogue to that of a single slightly thicker PS layer (or a single overlay with the same thickness of 320 nm and higher refractive index) [10,26].

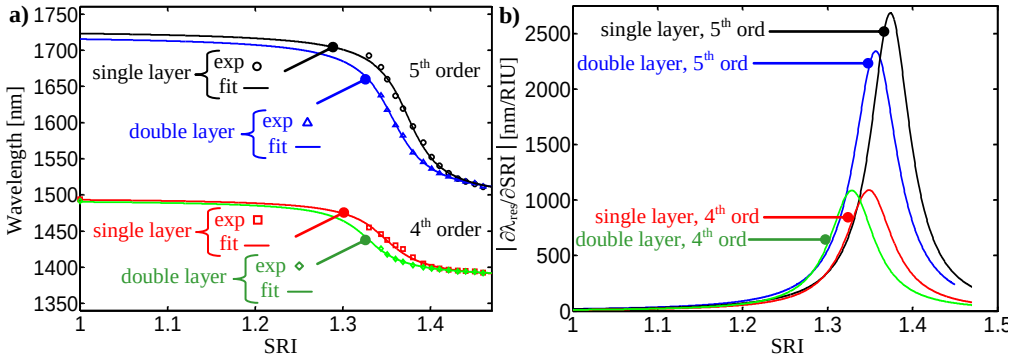

Fig. 3. a) SRI characterization in terms of attenuation bands minima position for the fourth and fifth cladding modes and for the single- and double-layer coated grating A; b) SRI sensitivity ($|\partial\lambda_{res}/\partial SRI|$) of the fourth and fifth cladding modes extrapolated from data reported in a).

The decrease in the peak sensitivity is less marked on the fourth order cladding mode than on the fifth order. It is also worth noting that for a fixed coating (single or double) the

#132072 - $15.00 USD Received 21 Jul 2010; revised 27 Sep 2010; accepted 27 Sep 2010; published 3 Jan 2011

transition index, i.e. the SRI corresponding to the peak sensitivity, is slightly bigger for higher order modes. Therefore, in order to tune higher order modes in full transition region for an SRI = 1.33 it is necessary a thicker overlay.

4. Biomolecular experiments

4.1 Covalent attachment of bioreceptors

In this paragraph we report biomolecular experiments carried out with grating A. In particular, dynamics of protein binding were continuously monitored through automated spectral acquisition of the attenuation bands related to the fourth cladding mode of the grating A. The LPG, coated with a double polymer layer as described in the previous paragraph and so tuned in transition region, was enlightened by a SLED (10 mW, 1550 nm central wavelength) and spectra were recorded each 7 seconds from a computer controlled OSA. Solutions were added and withdrawn from the bowl by careful manual pipetting. The volume of solution around the gratings was kept constant at about 3 mL. With reference to Fig. 4(a), (b) and grating A, we explain the single steps of the first experiment. At the beginning the coated grating was immersed into freshly prepared 4-(2-hydroxyethyl)-1-piperazineethanesulfonic acid buffer (HEPES, 0.01 M; Aldrich) in sterile double distilled water (ddH_2O) with 1-ethyl-3-(3-dimethylaminopropyl)carbodiimide (EDC, 0.004 M; Aldrich) and N-hydrosuccinimide (NHS, 0.01M; Aldrich) for about 30 minutes (I). This is a standard coupling chemistry used to crosslink proteins to surfaces exhibiting carboxyl groups [25]. Subsequently, the device was extracted from the NHS/EDC solution, immediately relocated in a clean bowl and submerged into 3 mL of fresh HEPES buffer solution (II). It is worth observing that each time the grating is extracted/submerged into the aqueous environment there is a sort of acclimation of the polymeric layer expressed through a quite fast red wavelength shift. A plausible explanation of this phenomenon will be sketched in the last paragraph. After signal stabilization, 1 mL of HEPES was gently withdrawn being sure that the device would be still completely covered by the liquid and then 1 mL of the SA (Mw = 58.6kDa; #S888 Invitrogen) solution was gently injected to reach a final concentration of 0.1 mg/mL (III).

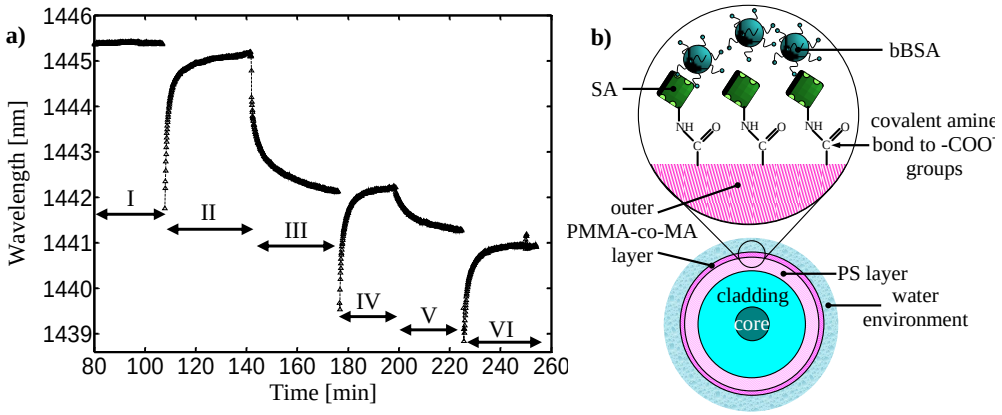

Fig. 4. (a)LPG sensorgram reporting the wavelength shift of 4th order cladding mode attenuation band during the immobilization procedure and following affinity-assay; (b) sketch of coated LPG interface with different biological agents used in the experiment.

Table 1. Salient data extracted from the biomolecular experiment

Step	Δλ [nm]	Δt (10-90%) [min]
SA (III)	≅3.1	≅17
bBSA (V)	≅0.9	≅15
wash (II)	≅3.4	≅8
wash (IV)	≅2.6	≅7
wash (VI)	≅2.1	≅6

#132072 - $15.00 USD Received 21 Jul 2010; revised 27 Sep 2010; accepted 27 Sep 2010; published 3 Jan 2011

At this point a kinetic due to formation of stable amine bonds between streptavidin and surface carboxyl groups started to be recorded. After 35 minutes, when the signal had reached a quite stable value the device was moved into clean buffer (IV). Beside the already mentioned acclimation dynamic it is important to note that the signal converges to a value very close to that reached at the plateau of the previous step (III). This means that proteins were stably attached to the surface without any tendency to be detached, on the contrary of what was happening in ref [10]. where the first layer of proteins was simply adsorbed. In addition, the covalent immobilization of the bioreceptor is faster than the adsorption procedure and so the preparation of the biosensor. When the bBSA (Mw = 66.5kDa; #A8549 Aldrich) of final concentration 0.1 mg/ mL was added to the bowl, a second dynamic was observed related to the affinity binding of this protein to SA (V). Again after washing the protein was completely retained (VI). A small blue shift of the baseline in this last step is most likely due to impurities collected in the extraction from the solutions. Salient data are summarized in Table 1. It was already observed in ref [10]. that the bulk refractive index of the considered protein solutions differs from that of the buffer without proteins for less than the accuracy of an Abbe refractometer. On the other hand the wavelength shifts measured here, given the sensitivity of the device, correspond to an effective refractive index change of $2\text{-}3 \times 10^{-3}$. Therefore we can roughly estimate that the effect of the bulk refractive index change has an influence on the amplitude of the dynamics for few points per cent (also evident from Fig. 4.a step III-IV). Moreover, as the unbound proteins in solution are completely eliminated at each washing step, the wavelength shift between the plateau levels before the protein injection and after washing gives an information only about the condensed layer of proteins on the surface of the LPG.

Excess proteins are used to ensure that unspecific adsorption or sedimentation in the bowl could excessively reduce the actual proteins concentration in the solution. For what concerns the different amplitude of the $\Delta\lambda$ for the two protein monolayers, which after all have similar dimensions and RI [28], it could be related to the non-linear transfer characteristic of the device, also highlighted by the decreasing signal excursion in the acclimation phases during subsequent immersions. Another reason for the uneven shifts is most likely due to the fact that the direct covalent attachment of bioreceptors on a sensor surface, while improving the stability of the immobilization, can reduce their capture efficiency. An interesting observation from the time responses of the different kinetics collected in Table 1 is that, also from this point of view, the two phenomena, protein binding and polymer acclimation, can be well distinguished. In further developments of this work, a microfluidic system incorporating the device should fix the acclimation and the impurity collection issues, as well as enable tests with smaller protein concentrations.

4.2 AFM characterization

In this paragraph, we briefly report an AFM analysis of double layer coated optical fibers in order to show the effectiveness of the outer PMMA-co-MA layer in the immobilization procedure of bioreceptors (in our case SA). The images were taken on dry samples in air. The employed apparatus is an AFM-SNOM system, the Multiview 1000 by Nanonics Imaging Ltd., integrated with a conventional optical microscope by Olympus, and equipped with cantilevered optical fiber probes (Nanonics Imaging Ltd.) with a nominal spring constant 1 N/m and a tip radius of curvature 5 nm. All images were obtained using tapping mode operation and a set-point 80% of the free amplitude oscillation. AFM data were not filtered, although the topographic image data were flattened using a first or second order line fit to eliminate sample tilt using WSxM free software downloadable at http:www.nanotec.es.

Figures 5(a), (b) show a topography image ($2\text{x}2\ \mu m^2$, 2D and 3D respectively) of a PMMA-co-MA coated optical fiber. This fiber was incubated, without applying NHS/EDC chemistry, in a solution of SA in HEPES for the same time and at the same concentrations used for the real-time biomolecular tests reported in paragraph 4.1. Afterwards the fiber was rinsed in ddH_2O and then dried with dry nitrogen. This step had the purpose to show that there

#132072 - $15.00 USD Received 21 Jul 2010; revised 27 Sep 2010; accepted 27 Sep 2010; published 3 Jan 2011

is any unspecific adsorption of proteins on the polymer surface if a specific coupling chemistry is not applied.

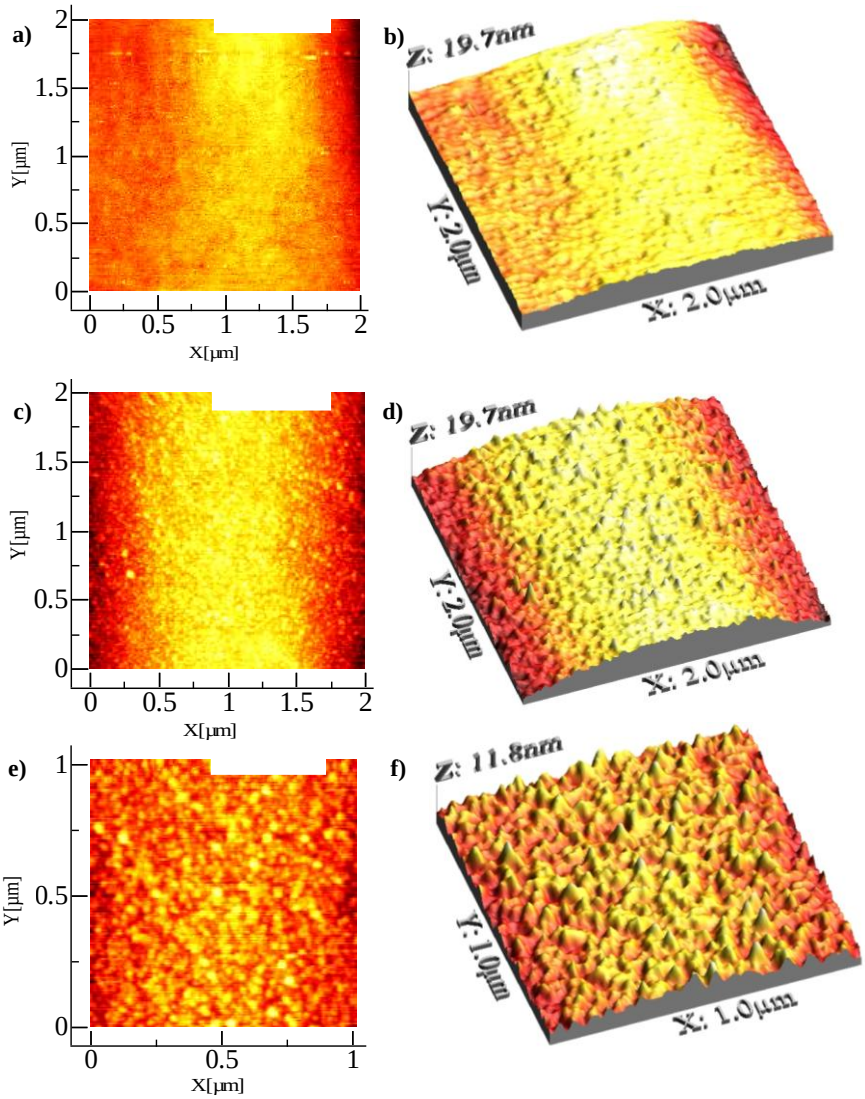

Fig. 5. (a) and (b) are 2D and 3D, respectively, height images of PMMA-co-MA coated optical fiber without covalently attached SA; (c) and (d) are 2D and 3D, respectively, height images of the coated fiber after covalent immobilization of SA; (e) and (f) are 2D and 3D, respectively, height images of immobilized protein on the coated fiber on a smaller area of 1x1 μm^2.

In fact, in the figure it can be noticed that except for the curvature (due to the underlying fiber) the surface appears to be quite flat with a roughness (RMS) of only 2.19 nm. The same fiber was then treated with the NHS/EDC chemistry for the same time and at the same concentrations of the biomolecular tests reported in paragraph 4.1, then it was again incubated in SA. Figures 5(c),(d) show a topography image (2x2 μm^2, 2D and 3D respectively) of the fiber after this second type of treatment. In this case the roughness was found to be 3.45 nm. An even more detailed picture of the surface is reported in Figs. 5(e),(f) (2D and 3D) where the scanned region was just 1x1 μm^2. The images show nicely and densely packed globular features that quite uniformly cover the fiber surface. This analysis was necessary to

#132072 - $15.00 USD Received 21 Jul 2010; revised 27 Sep 2010; accepted 27 Sep 2010; published 3 Jan 2011

understand if the relatively small concentration of carboxyl groups (1.6%) in the co-polymer could be satisfactory in terms of immobilized biological material.

From the topography image it is possible to retrieve an average height of the globular features of about 5 nm, which is consistent with the expected thickness of the biological coating considered the height SA. The cross-sectional analysis revealed diameters of the globular features of few tenths of nanometers up to more than 50 nm. Although the proteins considered here should have much smaller diameters it is well known that the topography images in the lateral dimensions suffer of the convolution effect produced by the AFM tip. Moreover a certain degree of protein clustering cannot be excluded. However, the dimensions here reported well agree with those of other AFM studies [29].

4.3 Discussion

First of all it is honest to mention that the dip-coating technique does not allow for a such accurate control of the thickness as the ESA technique [6,8,11,12]. Therefore slight parametric variations in the deposition process could seriously affect the reproducibility of the fabricated devices. Nonetheless the dip-coating can be made more reproducible by increasing the controlled parameters. The use of a chamber with controlled atmosphere, an antivibrating table and the control of the density and viscosity of the solutions can greatly improve the process reliability. Finally, given the high sensitivities achieved with the device tuned in transition region, a small detuning from the peak sensitivity due to parametric variations of the overlay does not constitutes a great problem. In fact, the sensor could be properly calibrated with suitable reference saline solutions.

It is useful at this point to consider in more detail the several reasons for using a double-layer approach to the concurrent tasks of sensitivity optimization and functionalization of the LPG. In fact, one may wonder why to not directly functionalize the surface of a HRI overlay or to not use a single layer of a bulk- functionalized material. A general consideration is that by modifying surfaces, one can confer to a material with useful bulk properties the suitable surface properties. First of all, while PS layers deposited by DC, in light of their higher refractive index than the cladding and low optical losses, have shown to be a suitable choice to put LPGs to work in transition mode, at the same time it is not trivial to find surface functionalization techniques providing high density of carboxyl groups without affecting the morphological and optical characteristics of the overlay and in particular without introducing optical losses.

On the other side, the use of a single PMMA-co-MA layer has several disadvantages. First of all, although the PMMA-co-MA has a slightly higher RI than the cladding that enables the modal transition phenomenon, nonetheless it has a much lower RI than PS. This would result both in a thicker overlay (approx. 2.7 times thicker than a single PS overlay) to tune the LPG in the transition region and in a less steep transition region (peak sensitivity approx. 2.3 times lower than with a single PS overlay), as determined from a numerical analysis based on the theory reported in [6]. Thicker overlays to be deposited require high density solutions (up to 20% by weight of PMMA-co-MA) which can be cumbersome to prepare. Secondly, PMMA-co-MA absorbs a small amount of water which anyway can cause a considerable change of the optical properties of the polymer as we are going to show. This inconvenient drawback can cause undesired detuning of the attenuation band from the transition region during immersion in the test environment. In light of these arguments it is convenient to use a double-layer approach and minimize the thickness of the outer PMMA-co-MA layer. In this way high sensitivity in transition region, low optical losses, minimal perturbation of the optical design and high density of surface carboxyls are ensured. We can estimate that with our double layer design we have held the loss of sensitivity (due to the use of the polymer with relatively low refractive index) with respect to a single layer design (having the same tranistion index) to only −3.6%.

Another important consideration to point out is that the PMMA-co-MA polymer used in this work has a carboxyl content (1.6%) which is the functional group used for covalent attachment of proteins. It is reasonable to assume that due to the hydrophilic nature of this

#132072 - $15.00 USD Received 21 Jul 2010; revised 27 Sep 2010; accepted 27 Sep 2010; published 3 Jan 2011

pendant group, when the secondary layer is deposited in the form of thin film atop the hydrophobic PS layer, there should be a preferential orientation of the carboxyls toward the outer surface in contact with the surrounding environment. Although a direct characterization of the surface density of carboxyl groups was not performed, atomic force microscopy (AFM) imaging (discussed in paragraph 4.2) showed a dense and uniform protein coverage after covalent attachment. Obviously, the percentage of the protein covered surface could be increased by using a co-polymer with a higher feed ratio. However this would not necessarily mean better performance. First of all, higher content of carboxyl groups would increase the water uptake in the overlay entailing difficulties in the tuning of the working point in transition region. An excessive swelling of the secondary layer could even cause its detachment from the underlying hydrophobic PS. Secondly, protein overcrowding results in reduced bioreceptor capture efficiency.

Finally, it is worth to remark that the slight decrease in the peak sensitivity of the coated LPG due to the additional overlay with lower refractive index than PS can be easily compensated through a careful optical design as demonstrated in the next section.

5. Sensitivity optimization

In this section, we demonstrate that a careful design of the final device provides a useful tool for an efficient sensitivity optimization. Moreover we address several issues, only briefly mentioned in the previous paragraphs, concerning the PMMA-co-MA interaction with water. There are several parameters that can be tuned in order to achieve an optimal biosensor design, among them the easier to change are the grating period, the PS overlay thickness, the PMMA-co-MA overlay thickness and the percentage of methacrylic acid in the PMMA co-polymer. Without pretending to give a comprehensive analysis of all possible parameter variations we identify the guidelines for an improved biosensor performance.

5.1 PMMA-co-MA interaction with water

As already discussed above a general method to improve the performance of a LPG-based sensor is to interrogate an higher order cladding mode. To this purpose in the following we report experiments carried out with grating B that was chosen for its shorter period (Λ = 380 μm) compared to grating A (Λ = 460 μm), enabling observability of the sixth order cladding mode in transition region. Moreover, it is worth noting that only commercial gratings were used, while a careful LPG design could ulteriorly boost the performances.

Figure 6(a) shows the spectral position of the attenuation band related to the fifth cladding mode for the bare device and for the coated device (in air). The DC deposition parameters were the same as for the grating A except for the concentration of the PS solution which was in this case increased to 9.7% (w/w). This was necessary to achieve a thicker PS layer (reasonably comprised between 320 and 370 nm [10]) and tune the sixth order cladding mode in transition region. In fact, in the same plot it is also reported the presence of the sixth order cladding mode attenuation band in transition region (around 1578 nm, violet) with water as surrounding medium. With reference to this case we propose an interpretation of the observed phenomenology regarding the polymer-water interaction without pretending to give an exhaustive explanation which is, in fact, beyond the scope of this work. The spectra were acquired on a smaller wavelength range while the LPG was fed by a superluminescent light emitting diode (SLED, 10 mW, 1550 nm central wavelength). In this way a faster scan time could be set allowing real-time monitoring of the kinetics of polymer-water interactions that are reported in Fig. 6(b).

When the coated LPG is immersed in water (3 mL) for the first time a water absorption kinetic consisting of a red wavelength shift is observed (from 1578.2 to 1589.9 nm). This was expected since it is widely known that PMMA is slightly hydrophilic and PMMA-co-MA is expected to have even higher levels of water uptake owing to the carboxyl groups content. Samples were acquired each 7 seconds in the first 10 minutes and afterwards each 60 seconds since the constant time of the phenomenon was observed to be slow enough. It is interesting to point out that the absorption dynamic increased its rate of change after a lag time of a couple

#132072 - $15.00 USD Received 21 Jul 2010; revised 27 Sep 2010; accepted 27 Sep 2010; published 3 Jan 2011

of minutes, which is a typical effect of a diffusion behavior. After about 150 minutes the kinetic reached the plateau level.

The net observed effect of water absorption is that of reducing the refractive index of the outer layer and it is most likely due to a density decrease accompanied by a minor swelling effect. Again in Fig. 6(a) it is shown the considered attenuation band after the water uptake to highlight the absence of fading (blue color). After this step, the device was extracted from the water, relocated in a clean and empty bowl, the acquisition was restarted with a scan time of 7 seconds and the device was again submerged by 3mL of water.

This time the observed kinetic started from a higher wavelength compared to that of the first dynamic, but lower than the plateau wavelength of the first dynamic. This is consistent with an hypothesis of a PMMA-co-MA overlay with reduced refractive index. In this system, it is reasonable to assume that the water is absorbed through hydrogen bond at hydrophilic sites rather than through infiltration in free spaces as already reported for PMMA modified with hydrophilic functional groups [30]. Therefore there should be a certain amount of absorbed water that is strongly retained in the polymer and not released during extraction from the water environment. Coming back to the analysis of the kinetic, it reached a quite stable plateau level very close to that of the previous dynamic in few minutes. This second type of dynamic is most likely due to an effect of structural relaxation of the hydrated polymer layer, also having as predominant effect a decrease of the overlay RI. From these observation we could conclude that the first observed dynamic is the integral sum of the water absorption and a gradual structural relaxation depending on the actual level of absorbed water. Instead the second dynamic is mainly due to an elastic structural relaxation, being the overlay already saturated by water. Confirmation of the reliability of this assumption is provided by a third experiment. If the grating is pulled out of the bowl and for the third time relocated and submerged by the water the fast red wavelength shift is repeated with a high degree of similarity. The different starting wavelength in this case is just related to the manual process of water injection that cannot ensure an instantaneous coverage of the whole LPG.

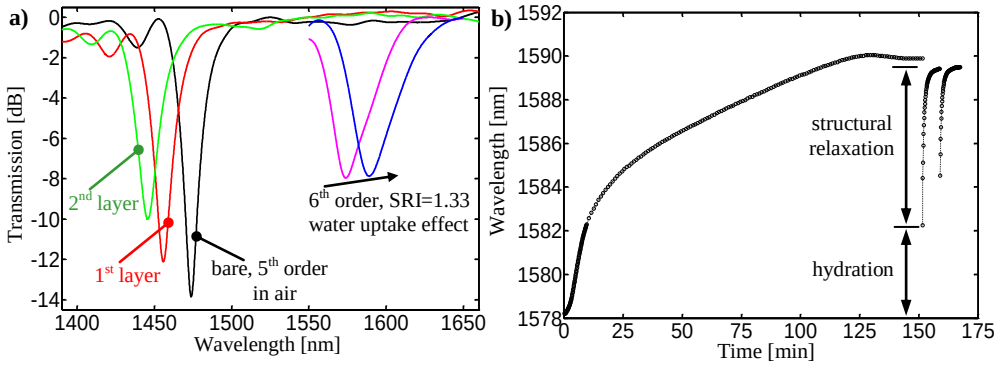

Fig. 6. a) Effect of the overlays deposition on the fifth order cladding mode attenuation band of grating B in air, position of the attenuation band related to the sixth order cladding mode when the grating is immersed in water (violet) and band shift due to water absorption (blue); b) Kinetic of the attenuation band of the sixth order cladding mode as a consequence of water-polymer interaction in different consecutive immersions.

The study of the interaction of the PMMA-co-MA with water leads us to conclude that the refractive index decrease of the secondary layer in the test environment should be necessarily taken into account when designing the device to work in transition region. It would be preferable to reduce the thickness of the secondary layer bearing in mind the robustness of double layer system. Another parameter affecting the water uptake effect is the percentage of methacrylic acid in the co-polymer, the higher the carboxylic groups content the higher the water uptake. Although one may think to increase this percentage to have a more dense bioreceptor immobilization, nonetheless the AFM analysis reported in paragraph 4.2 suggests that the seemingly small percentage used (1.6%) should be already satisfactory from this point

#132072 - $15.00 USD Received 21 Jul 2010; revised 27 Sep 2010; accepted 27 Sep 2010; published 3 Jan 2011

of view. Finally, it is worth remarking that a step of layer hydration is needed, after performing the deposition and the solvent evaporation, in order to have a repeatable sensor behaviour and minimize baseline drifts.

5.2 Improved biomolecular experiments

The grating B was used in these experiments in order to show a biomolecular detection carried out with improved sensitivity and in an attempt to work in a more linear region of the transfer characteristic. In fact higher order modes not only ensure higher sensitivity but also higher "bandwidth" (ΔSRI_{3dB}) of the sensitivity function [26] which in turn means improved linearity of the device response. The LPG was coated with a double layer as already described above. After surface activation with NHS/EDC chemistry and immobilization of a first layer of SA (incubated for about 30 min), multiple alternate bBSA/SA affinity assays were carried out. Therefore this time it was possible to exclude that uneven wavelength shifts could be due to a different type of binding (covalent rather than affinity). With reference to Fig. 7 we list in the following the single steps of the second experiment, performed with the same procedure and solutions concentration as described in paragraph 4.1: bBSA affinity binding (I), HEPES wash (II), SA affinity binding (III), HEPES wash (IV), bBSA affinity binding (V), HEPES wash (VI), SA affinity binding (VII), HEPES wash (VIII). The reported wavelength shifts were obtained by a centroid analysis of the acquired spectra rather than simply retrieving the transmission minimum that, in the case of a wide attenuation band, gives more scattered data. Salient data are summarized in Table 2. It is important to underline that in this experiment the SA (step III and VII) is collected on the sensor surface via affinity binding, while the previous experiment (Fig. 4 and Table 1) reports the covalent attachment on the sensor surface, this explain the quite different constant time of the SA binding kinetic.

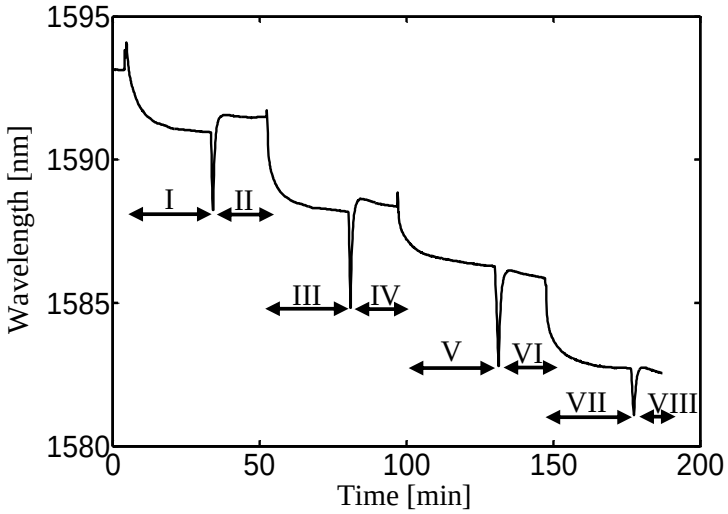

Fig. 7. LPG sensorgram reporting the wavelength shift of 6th order cladding mode attenuation band during multiple affinity-assays.

Table 2. Salient data extracted from the optimized biomolecular experiment

Step	Δλ [nm]	Δt (10-90%) [min]
bBSA (I)	≅2.2	≅13
SA (III)	≅3.3	≅9
bBSA (V)	≅2.1	≅18
SA (VII)	≅3.2	≅10

It is useful to do some observations which may help to better understand the reported sensorgram. Before each injection of proteins and consequent beginning of binding dynamic

#132072 - $15.00 USD Received 21 Jul 2010; revised 27 Sep 2010; accepted 27 Sep 2010; published 3 Jan 2011

(steps I, III,V,VII) it can be noticed a small spike towards higher wavelengths. This effect is due to the withdrawn of 1 mL of buffer solution before the injection of the protein solution and it is most probably related to a change in the equilibrium condition of the hydrated polymer overlay. However the total volume of solution is always restored with the injection of 1 mL of protein solution. The binding dynamics were monitored for about 30 min, that is a reasonable incubation time to achieve a full coverage of our surface. The steps II, IV, VI and VIII are the dynamics of the polymer acclimation in the aqueous environment for each time the grating is immersed in the buffer solution without the proteins. A time slot of 15 min was observed to produce a quite stable baseline before the subsequent injection of protein solution. The plateau wavelength reached in the washing steps was measured to differ from that at the end of the binding kinetics for an average value of 0.4 nm. This can be partially explained considering a small fraction of proteins dissociated from their binding. However it should be also recognized that the manual injection of the liquids and the acclimation of the polymer in the aqueous environment can affect the accurate reproducibility of the measurements. It will be therefore essential in further developments of this work to incorporate the sensor in an automated microfluidic system. This would be certainly helpful to fix some of the observed anomalies.

It is worth stressing again that the concentration of protein solutions used in the experiments was intentionally chosen to achieve a full coverage of the LPG sensor. Therefore the measured wavelength shifts (Table 2) are related to the formation of protein monolayers. Even though a scale of concentrations was not reported here for the already mentioned uncertainty associated to the manual injection procedure, however some considerations on the expected limit of detection of the proposed configuration can be done. Considering that a relatively low order cladding mode (5th order for example) tuned in transition region for SRI = 1.33 shows a refractive index sensitivity of approx. 2000 nm/RIU and that commercial spectrometers with resolution of 10 pm are readily available, a refractive index resolution of the device approaching 5×10^{-6} is expected. Therefore limits of detections close to those reported for fiber optic surface plasmon resonance sensors (5 pg/mm^2) [31] are reasonably attended. However we can foresee significant performance improvements by using higher order cladding modes of LPGs.

6. Conclusions

In this work we reported LPGs coated with multiple layers of transparent polymers for biosensing applications. The dip-coating technique and an original solvent/non-solvent strategy were exploited for the deposition of the thin films. The multilayer approach was developed in order to decouple the problem of the optical design, aimed to a highly sensitive device to SRI changes, from that of the outer layer functionality. In particular, polystyrene was used as HRI material in the form of a thin film of few hundreds nanometers to tune the working point of the device in transition region. This allowed to achieve a SRI sensitivity ($|\partial\lambda_{res}/\partial SRI|$) largely exceeding one thousand of nanometers per refractive index unit (depending on the interrogated cladding mode). A commercial PMMA co-polymer containing functional carboxylic groups was deposited as secondary coaxial coating of few tens of nanometers in a trade-off between minimized impact on the optical design and sufficient robustness. The covalent immobilization of bioreceptors (SA) to the outer functional surface was proven by means of real-time monitoring of the attenuation bands shift and confirmed through AFM analysis. An advanced design of the device involving higher order modes showed that it is possible to regain the little loss of sensitivity due to the outer layer, characterized by a relatively low refractive index, while improving at the same time the linearity of the response. This feature was proven by performing the detection of the building up of multiple protein layers (SA/bBSA) on the sensor surface. The limit of detection of the proposed biosensor could be estimated to be around 5 pg/mm^2, which is comparable to other competing fiber optic label-free technologies. However the wide design margins offered by the mode coupling in LPGs let to foresee further considerable improvements.

#132072 - $15.00 USD Received 21 Jul 2010; revised 27 Sep 2010; accepted 27 Sep 2010; published 3 Jan 2011